Zoological Journal of the Linnean Society, 2025, **203**, zlae142
https://doi.org/10.1093/zoolinnean/zlae142
Advance access publication 2 January 2025
Original Article

OXFORD

Original Article

Will the real invasive snail please stand up? A phylogenetic reconsideration of *Paralaoma servilis* (Shuttleworth, 1852) (Gastropoda: Stylommatophora: Punctidae)

Jeffrey C. Nekola[1], Fred J. Brook[2], Junn Kitt Foon[3,4], Veronika Horsáková[1], Yasuto Ishii[5], Frank Köhler[3], Eva Líznarová[1], Markéta Nováková[1], Takumi Saito[1,6], Rodrigo B. Salvador[7,8], Michal Horsák[1]

[1]Department of Botany and Zoology, Masaryk University, Kotlářská 2, CZ-611 37 Brno, Czech Republic
[2]PO Box 1652, Nelson 7040, New Zealand
[3]Australian Museum Research Institute, Australian Museum, 1 William Street, Sydney NSW 2010, Australia
[4]School of Science, Western Sydney University, Hawkesbury Campus, Richmond NSW 2753, Australia
[5]Department of Biology, Faculty of Science, Tohoku University, 6-3 Aramaki Aza-Aoba, Aoba-ku, Sendai 980-8578, Japan
[6]Department of Ecological Science, Vrije Universiteit Amsterdam, De Boelelaan 1085, 1081 HV, Amsterdam, the Netherlands
[7]The Arctic University Museum of Norway, UiT—The Arctic University of Norway, Lars Thørings veg 10, 9006 Tromsø, Norway
[8]Zoology Unit, Finnish Museum of Natural History, University of Helsinki, Pohjoinen Rautatiekatu 13, 00100 Helsinki, Finland

*Corresponding author. E-mail: nekola@sci.muni.cz

ABSTRACT

We reconsider the biodiversity and biogeography of *Paralaoma servilis*—believed to be one of the most globally invasive exotic land snails—through integrative empirical revision. Phylogenies obtained from nDNA (*ELAV*, ddRAD genomics) and mtDNA (*COI*) demonstrate that the current classification is in error, with there being at least five distinct species within *P. servilis s.l.* The *P. servilis* group as interpreted here thus includes: *P. servilis*, inferred to be native to south-western Pacific Rim with an adventive distribution minimally spanning North America, Europe, and the Macaronesian islands of the eastern Atlantic Ocean; *P. amblygona* (Reinhardt, 1877), native to Honshu, Japan; *P. borealis* (Pilsbry and Y. Hirase, 1905), native to Hokkaido, Japan along the Pacific Rim to the SW North American mountains; *P. caputspinulae* (Reeve, 1852), native to New Zealand and Lord Howe Island; and *P. morti* (J.C. Cox, 1864), native to south-eastern Australia. Within *P. servilis*, invasiveness appears limited to a single clade that may have arisen along the California coast. The work presented here is a reminder that taxonomic concepts that have not been subjected to empirical vetting can generate poor biodiversity perspectives and non-optimal conservation strategies when native species are treated as exotics.

Keywords: geometric morphometrics; integrative taxonomy; ddRAD genomics; introduced species

INTRODUCTION

As biodiversity must be known before it can be protected, it is frequently stated that taxonomy is the foundation of biodiversity science (Costello *et al.* 2015, Conix 2019). But what happens when this taxonomy is wrong? How is our ability to protect biodiversity and generate optimum conservation strategies inhibited by the fact that traditionally recognized land snail species often do not survive confrontation with empirical data (Nekola and Horsák 2022)? What if distinct, native, non-invasive entities have been incorrectly lumped into a putative invasive taxon?

We consider this through *Paralaoma servilis*, which has one of the most convoluted nomenclatural histories of any land snail: since its first attempted naming—as *Helix* (*Helicella*) *pusilla* R.T. Lowe, 1831 (which was preoccupied)—this entity has been assigned to no fewer than 57 *nomina* within well over a dozen genera, including *Microphysa*, *Patula*, *Pleuropunctum*, *Punctum*, *Radioconus*, *Radiodiscus*, *Tachyphasis*, *Toltecia*, *Trachycystic*, and *Zilchogyra* (Roth 1986, Gittenberger *et al.* 2020, MolluscaBase 2024). A reason for this profound level of confusion is that it apparently ranges across all continents except Antarctica (e.g. Pilsbry 1948, Hausdorf 2001, Rosenberg

Received 3 June 2024; revised 23 August 2024; accepted 26 September 2024

and Muratov 2005, Rumi *et al.* 2010, Pokryszko *et al.* 2011, Boxnick *et al.* 2015), with taxonomists across its many far-flung outposts generally having categorized it as a native species (Christensen *et al.* 2012, Gittenberger *et al.* 2020). *Paralaoma servilis* is now thought to be among the most widespread invasive land snails (Gittenberger *et al.* 2020), with significant range expansions currently underway across Europe (Hausdorf 2023), eastern North America (Steury and Pearce 2014), and southern South America (Virgillito and Miquel 2013). Its current spread appears at least in part related to commercial transport of landscaping plants, in particular *Eucalyptus* in South America (Hausdorf 2023) and bamboo in Europe (Schmid 2002, Welter-Schultes 2012).

The original range of this species remains obscure, however. While some contend that centuries of accidental translocations have made it impossible to identify (Schütt 2001, Schmid 2002), a number of authors have postulated a New Zealand or Australia origin based on ranges of other native members of the genus, along with the presence of apparently similar fossil shells extending back to the Miocene (Price and Webb 2006, Marshall and Worthy 2017). Roth (1986: 25), however, concluded that because of its occurrences in remote montane habitats ranging from Alaska to New Mexico, it was also 'evidently indigenous' throughout much of western North America. Pleistocene fossil shells have also been reported from the Sacramento Mountains of southern New Mexico (Metcalf 1997), where modern populations persist to this day (Dillon and Metcalf 1997). And, even within its potentially invasive California coast occurrences, it seldom co-occurs with other exotics but is frequently found with local endemics of conservation importance (Pilsbry 1948, Nekola *et al.* 2018).

What does this species represent? Is it a highly invasive pest that originated in New Zealand or Australia that may be homogenizing biodiversity across the globe? Or is it also native outside of the south-west Pacific? Perhaps the issue lies in conventional taxonomic opinion: if *Paralaoma servilis* is not a single species but rather multiple entities, then both statements could be correct. Sadly, these competing hypotheses have never been empirically assessed because prior taxonomic decisions were solely based on qualitative conchology, which is especially limiting when shells are simple with apparently few obvious diagnostic traits. Genital anatomy is also likely to be uninformative, as is the case in many microsnails (Martínez-Ortí *et al.* 2007, Pokryszko 1987).

This study attempts to understand the taxonomy and biogeographic history of *Paralaoma servilis* through empirical integrative confrontation of current taxonomic hypotheses. Our scale is global, with studied populations ranging from Australia and New Zealand along the Pacific Rim to western North America, and then east to south-eastern North America, the Macaronesian Islands of the eastern Atlantic, and, finally, the European mainland. We subject this material to not only standard polymerase chain reaction (PCR) amplification followed by Sanger sequencing, but also single nucleotide polymorphism (SNP) genomics along with associated conchometric and geometric morphometric comparisons. From this we determine the number of biologically supported species, identify which race is globally invasive, and document how these various entities can be morphologically distinguished. We also reconsider the likely origin and timing of its global conquest.

MATERIALS AND METHODS

Specimen selection and DNA extraction

For genetic analysis, specimens of *Paralaoma servilis*, its putative junior synonyms and other morphologically similar taxa were sourced from a total of 40 populations from Australia, Lord Howe Island, Aotearoa/New Zealand, North America, Japan, Europe, and associated Macaronesian Islands (Table 1, Fig. 1). These included specimens of *Paralaoma morti* and *Paralaoma annabelli* Shea and O.L. Griffiths, 2010 from south-eastern Australia, *Paralaoma caputspinulae* from New Zealand, an unnamed *Paralaoma* from New Zealand, and two taxa currently attributed to the genus *Punctum*: *Punctum amblygonum* from Honshu and *Punctum boreale* from Hokkaido. We also included *Punctum conspectum conspectum* and *P. conspectum alleni* from North America, which had previously been synonymized into *P. servilis* (MolluscaBase 2004). Although many other Australasian punctid species have been attributed to *Paralaoma*, in New Zealand, at least, this genus has been indiscriminately used for a diverse group of uncoloured punctids that differ substantially from *P. caputspinulae* and the type species of the genus, *Paralaoma raoulensis* Iredale, 1913. Preliminary *COI* sequence data for some of these, including '*Paralaoma*' *lateumbilicata* (Suter, 1890), '*P*.' *pagoda* Climo, 1973, '*P*.' *regia* A.W.B. Powell, 1948, '*P*.' *sericata* (Suter, 1890), and '*P*.' *serratocostata* (W.H. Webster, 1906) demonstrate their deep, extra-generic divergence from *P. caputspinulae* (Fred Brook, unpublished data).

To allow for specific *nomena* to be accurately tied to particular clades, we have analysed material from the type localities of: *Paralaoma servilis* (Tenerife, Canary Islands), *Paralaoma caputspinulae* (New Zealand), *Paralaoma morti* (Sydney, Australia), *Punctum boreale* (Akkeshi, Kushiro, Japan), *Punctum amblygonum* (Tokyo, Japan), and *Punctum conspectum conspectum* (San Francisco, California). For *Punctum conspectum alleni*, the nearest available material to the Clackamas County, Oregon TL was from Stites, Idaho, approximately 525 km distant. Where possible we have included material from across the known geographic and ecological ranges of each taxa. *Miselaoma sinistra* was used as an outgroup.

Genomic DNA was extracted across the three participating laboratories using different kits and their associated protocols: E.Z.N.A. Mollusc DNA Kit (Omega BioTek) for work done in the Czech Republic and the QIAGEN DNA extraction kit for animal tissues for work done in Australia and New Zealand. These extractions have been archived in their respective laboratories at –80°C. Specimens of *Paralaoma hottentota* (Melvill and Ponsonby, 1891) from Africa (presently considered a synonym of *P. servilis*) and *P. servilis s.l.* from South America could not be included because of failed DNA extraction.

PCR amplification and Sanger sequencing

PCR amplification was performed for one mitochondrial (cytochrome *c* oxidase subunit I—*COI*) and one nuclear (embryonic lethality and abnormal visual system intron 8—*ELAV*) loci based on standard amplification protocols (Foon *et al.* 2023, Nekola

Table 1. Specimens used in genetic analyses. *Nomena* represent the earliest available within each *ELAV* and ddRAD-Seq identified species-level clade. Specimens collected within 500 km of the type locality for that *nomen* are preceded by '*'. Collections were sourced from AM: Australian Museum (Sydney, Australia); NMNZ: Museum of New Zealand Te Papa Tongarewa (Wellington, New Zealand); OZD: University of Otago (Dunedin, New Zealand); JCN: Jeff Nekola collection; Horsák: Michal Horsák collection; Coles: Brian Coles collection.

Taxon/Location	Latitude/Longitude	Collection Date	Collection	Specimen Accession #	ddRAD-Seq	Code	GenBank Accession #	
							COI	*ELAV*
Miselaoma sinistra (Gabriel, 1930)								
Australia								
New South Wales								
Kosciuszko NP, Goodman's Gully	35.674 S., 148.483 E.	24 January 2021	AM	C.589948		P75	PQ246669	PQ295359
Paralaoma amblygona (Reinhardt, 1877) **comb. nov.**								
Japan								
Honshu								
* Iwate: Geibikei Gorge	38.9873 N., 141.2557 E.	20 July 2012	JCN			P54	PQ246648	PQ295345
* Higashiyamacho	39.0049 N., 141.2602 E.	20 July 2012	JCN		SAMN43369184	H410	PQ246666	PQ295344
* Tōkyō: Renkoji, Tama	35.6325 N., 139.4677 E.	31 July 2012	JCN			H409	PQ246665	PQ295343
Paralaoma annabelli Shea and Griffiths, 2010								
Australia								
New South Wales								
* Bimberi Reserve, Cooleman Cave	35.625 S., 148.683 E.	21 January 2021	AM	C.589429		P60	PQ246653	PQ295349
* Bimberi Reserve, Magpie Flats	35.617 S., 148.672 E.	20 January 2021	AM	C.589836		P63	PQ246655	PQ295351
* Blue Mountains NP, Victoria Creek	33.574 S., 150.299 E.	1 November2020	AM	C.589839		P66	PQ246658	PQ295354
* Brindabella NP, Brindabella Road	35.366 S., 148.778 E.	28 January 2021	AM	C.589842	SAMN43369182	P69	PQ246660	PQ295356
* Mount York	33.558 S., 150.223 E.	31 October 2020	AM	C.589838		P64	PQ246656	PQ295352
* SE Forest NP, Cochrane Lake	36.567 S., 149.444 E.	1 June 2021				P72	PQ246662	PQ295348
Paralaoma borealis (Pilsbry and Hirase, 1905) comb. nov.								
Canada								
British Columbia								
Nechako Plateau	54.510 N., 126.315 W.	12 October 2015	NMNZ	M.328398		P28	PQ246624	PQ295321
Japan								
Hokkaido								
* Hami-Koshimizu	43.9335 N., 144.4439 E.	25 July 2012	JCN			P53	PQ246647	

Table 1. Continued

Taxon/Location	Latitude/Longitude	Collection Date	Collection	Specimen Accession #	ddRAD-Seq	Code	GenBank Accession #	
							COI	*ELAV*
* Lake Yudonuma	42.5877 N., 143.5358 E.	23 July 2012	JCN		SAMN43369183	P55	PQ246649	PQ295335
USA								
Alaska								
Falls Creek Wayside	60.9844 N., 149.5758 W.	13 August 2007	JCN	15 351		P43	PQ246637	PQ295334
California								
San Bernardino Co., Yellow Post Fen	34.2230 N., 116.9410 W.	28 September 2013	JCN	19 194		P40	PQ246634	PQ295333
Idaho								
Idaho Co., Stites South	46.0763 N., 115.9750 W.	5 September 2011	JCN	18 700		P44	PQ246638	PQ295336
(this population is <500 km from the *Punctum conspectum alleni* Pilsbry, 1919 type locality)								
Paralaoma caputspinulae (Reeve, 1852)								
Australia								
Lord Howe Island								
Neds Beach	31.518 S., 159.064 E.	5 July 2010	OZD	FB76		P31	PQ246631	PQ295340
Blinky Beach	31.543 S., 159.084 E.	2 September 2010	NMNZ	M.331229		P38	PQ246632	PQ295341
Valley of Shadows	31.528 S., 159.079 E.	9 October 2019	AM	C.583303	SAMN43369177	L542	PQ246667	PQ295338
Clear Place	31.529 S., 159.077 E.	9 October 2019	AM	C.583302	SAMN43369178	L543	PQ246668	PQ295339
New Zealand								
North Island								
* Waihau Bay, Wairua Stream mouth	38.240 S., 176.425 E.	7 November 2009	NMNZ	M.331228		P37		PQ295330
* Northland, Umuheke Bay	35.2608 S., 174.2944 E.	2 October 2018	OZD	FB48		P30	PQ246626	PQ295337
South Island								
* Canterbury, Gards Road	44.8134 S., 170.5189 E.	22 January 2021	NMNZ	M.331222		P33	PQ246627	PQ295322
* Southland, Colac Bay	46.362 S., 167.8847 E.		OZD	Paser-2		P27	MN792615	PQ295319
Paralaoma sp. NZ								
New Zealand								
South Island								
Canterbury, Lake Pukaki	44.1754 S., 170.1645 E.	14 December 1987	NMNZ	M.089606		P33b	PQ246664	

Table 1. Continued

Taxon/Location	Latitude/Longitude	Collection Date	Collection	Specimen Accession #	ddRAD-Seq	Code	GenBank Accession #	
							COI	*ELAV*
Paralaoma morti (J.C.Cox, 1864)								
Australia								
New South Wales								
* Jenolan Caves Reserve	33.808 S., 150.029 E.	8 November 2020	AM	C.586232	SAMN43369179	P58	PQ246651	PQ295346
***Jenolan Caves Reserve**	33.819 S., 150.023 E.	21 October 2021	AM	C.594138		P73	PQ246663	PQ295358
* Bimberi Reserve, Cooleman Cave	35.625 S., 148.683 E.	21 January 2021	AM	C.588429	SAMN43369181	P59	PQ246652	PQ295347
* Bimberi Reserve, Magpie Flats	35.617 S., 148.672 E.	20 January 2021	AM	C.589836		P61	PQ246654	PQ295350
* Kosciuszko NP, Yarrangobilly Caves	35.725 S., 148.491 E.	23 January 2021	AM	C.588490	SAMN43369180	P65	PQ246657	PQ295353
Paralaoma servilis (Shuttleworth, 1852)								
Australia								
New South Wales								
Hat Head NP, Ryans Cut S	31.127 S., 152.991 E.	28 April 2021	AM	C.589946	SAMN43369187	P71	PQ246661	PQ295357
Wollemi NP, Newnes Road	33.305 S., 150.118 E.	31 October 2020	AM	C.589835	SAMN43369185	P57	PQ246650	PQ295342
Blue Mountains NP, Victoria Creek	33.574 S., 150.299 E.	1 November 2020	AM	C.589840	SAMN43369186	P67	PQ246659	PQ295355
France								
Moréac	47.507 N., 2.720 W.	29 August 2008	Coles			P46	PQ246640	
Portugal								
Azores								
Ilha do São Miguel, Pópulo	37.750 N., 25.622 W.	10 November 2020	NMNZ	M.331224		P34	PQ246628	PQ295360
Ilha do Faial, Capelinhos	38.600 N., 28.819 W.	29 January 2020	NMNZ	M.331225		P35	PQ246629	PQ295317
Madeira								
Santa Cruz, Rua da Riberia	32.693 N., 16.804 W.	6 July 2016	Horsák		SAMN43369190	P45	PQ246639	PQ295320
Spain								
Tenerife								

Table 1. Continued

Taxon/Location	Latitude/Longitude	Collection Date	Collection	Specimen Accession #	ddRAD-Seq	Code	GenBank Accession #	
							COI	*ELAV*
* Ladera del Pico de las Flores	28.4316 N., 16.3901 W.		NMNZ	M.331226		P36	PQ246630	PQ295318
* Anaga Mts, Cruz del Carmen	28.532 N., 16.281 W.	19 April 2022	Horsák			P47	PQ246641	
* Teno Alto	28.205 N., 16.523 W.	18 April 2022	Horsák			P48	PQ246642	PQ295332
USA								
California								
Monterey Co., Pt Lobos Reserve	36.5215 N., 121.9519 W.	5 October 2013	JCN	19 272	SAMN43369188	P41	PQ246635	PQ295329
Santa Catalina Isl., Black Jack camp	33.3851 N., 118.4093 W.	2 February 2020	JCN	22 585		P39	PQ246633	PQ295325
San Diego Co., San Onofre beach	33.3775 N., 117.5682 W.	30 September 2013	JCN	19 207		P49	PQ246643	PQ295326
Engineer Springs	32.5916 N., 116.7627 W.	3 February 2020	JCN	22 589		P50	PQ246644	PQ295327
San Francisco Co., Presidio	37.794 N., 122.481 W.	15 March 2018	NMNZ	M.328399		P29	PQ246625	PQ295331
(*Punctum conspectum* (Bland, 1865) type locality)								
Sonoma Co., Bodega Bay	38.3492 N., 123.0629 W.	12 September 2013	JCN	19 186		P42	PQ246636	PQ295323
South Carolina								
Spartanburg Co., Spartanburg	34.9598 N., 81.9293 W.	28 August 2021	JCN	22 651	SAMN43369189	P51	PQ246645	PQ295324
Washington								
Thurston Co., SE Yelm	46.8709 N., 122.5561 W.	8 July 2021	JCN	22 609		P52	PQ246646	PQ295328

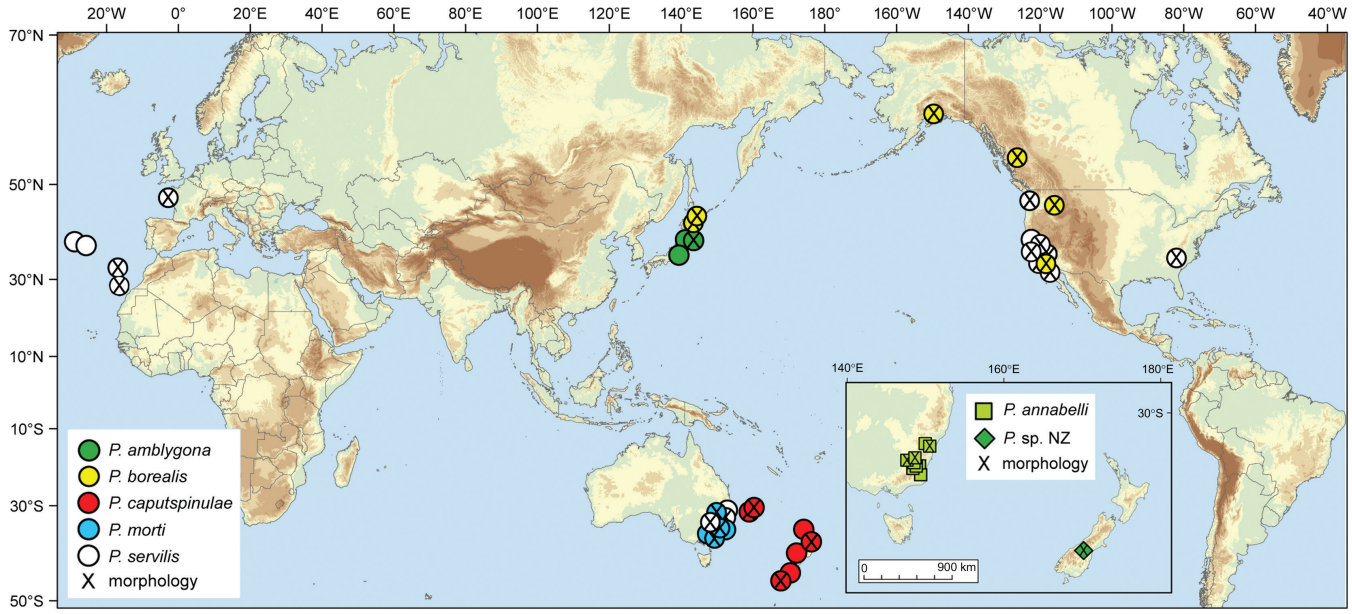

Figure 1. Location and verified identify of populations included in genetic and morphometric analyses.

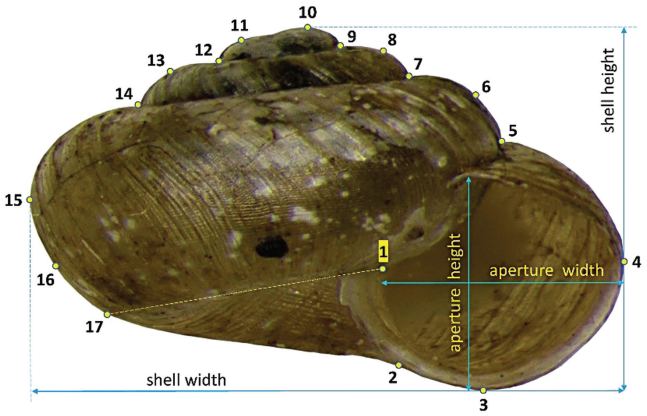

Figure 2. Measured shell parameters and landmark locations. Note that umbilicus width is not illustrated here, but represents the maximum distance of the inner wall of the body whorl as seen from the bottom.

et al. 2023). PCR products were cleaned (see: Horsáková *et al.* 2022) and sequenced in-house in Australia and New Zealand, and by the OMICS Core facility of SEQme s.r.o. in Brno, Czech Republic. Forward and reverse strands were assembled in ChromasPro 2.1.8 (Technelysium Pty Ltd) and checked by eye for potential errors. Amino acid translation of the *COI* fragment was used to check for erroneous stop codons. Sequence alignment was done with MAFFT v.7 using the Q-INS-i algorithm (Katoh and Toh 2008). All alignments were inspected for potential errors and corrected by eye, and are available upon request. GenBank accession numbers for all sequences used in phylogenetic analysis are provided in Table 1.

Phylogenetic reconstruction: PCR amplicons

Because of fundamental differences in hereditary mechanism, phylogenetic analyses were performed separately on mtDNA (*COI*) and nDNA (*ELAV*) sequences. To ensure robust and well-supported tree topology, we conducted two different reconstruction methods based on different analytical assumptions: Maximum likelihood (ML) analysis was performed in RAxML v.8.2 (Stamatakis 2014), using 500 search replicates and the GTR+G nucleotide substitution model. Internal node support was assessed via 1000 non-parametric bootstrap replicates (Felsenstein 1985). For Bayesian inference (BI), the optimum nucleotide substitution model was selected using jModelTest v.2.1.10 (Darriba *et al.* 2012) using the Bayesian information criterion. BI was performed in MrBayes v.3.2.6 (Huelsenbeck and Ronquist 2001), simultaneously running one cold and three heated MCMC chains for 10 000 000 generations, sampling every 1000 generations and with a burn-in of 25%. We ran four independent searches and used TRACER 1.6 (Drummond and Rambaut 2007) to assess convergence, checking that the effective sample sizes of all parameters were higher than 200 and standard deviation of split frequencies lower than 0.01. Topologically important nodes with support values above 60 for ML, and posterior probabilities above 70 for BI are shown in the final trees.

The ML tree was used to visualize phylogeny because both methods returned essentially identical tree topologies. We flipped/swapped resultant *ELAV* and *COI* subtrees to generate maximum visual correspondence. Genetically validated species were considered present when highly-supported reciprocally monophyletic clades were noted in *ELAV*. We identified cases of topological incongruence with *COI* and noted specimens that probably represent cases of mitochondrial introgression when *ELAV* sequence and diagnostic shell traits were for one taxon but *COI* sequence was from another.

Phylogenetic reconstruction: genome-wide SNPs

We also performed SNP analysis to reconstruct phylogeny using a broader segment of the nuclear genome. This was limited to 14 individuals spread across the six validated species-level groups (Table 1). Genome-wide SNPs were obtained through double

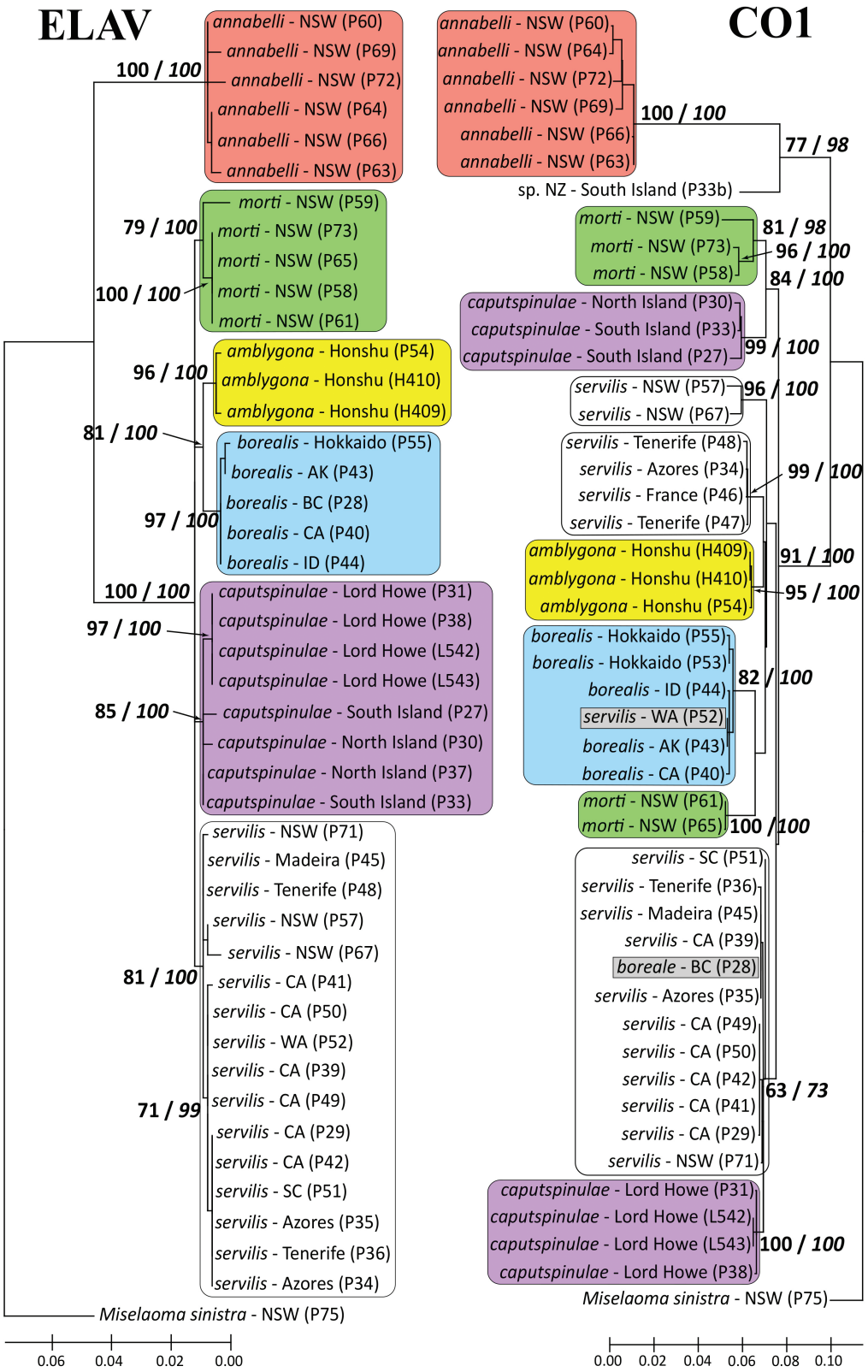

Figure 3. Maximum likelihood (ML) trees for *ELAV* (nDNA) and *COI* (mtDNA). Support values for important nodes are based on ML (left) and BI (right, italic). Instances where the *COI* sequence does not match the *ELAV* clade or identification based on diagnostic shell features are highlighted with a grey box, with the name representing the identification based on nDNA and morphometrics. Scale bars at the bottom represent maximum composite likelihood distances.

digest restriction-site associated DNA sequencing (ddRAD; Peterson *et al.* 2012). The sequencing library was constructed from approximately 50 ng of extracted genomic DNA using the EcoRI and MspI restriction enzymes. P1 and P2 adapters were ligated to the digested fragments. Following this, DNA fragments were multiplexed and purified using the Macherey–Nagel kit.

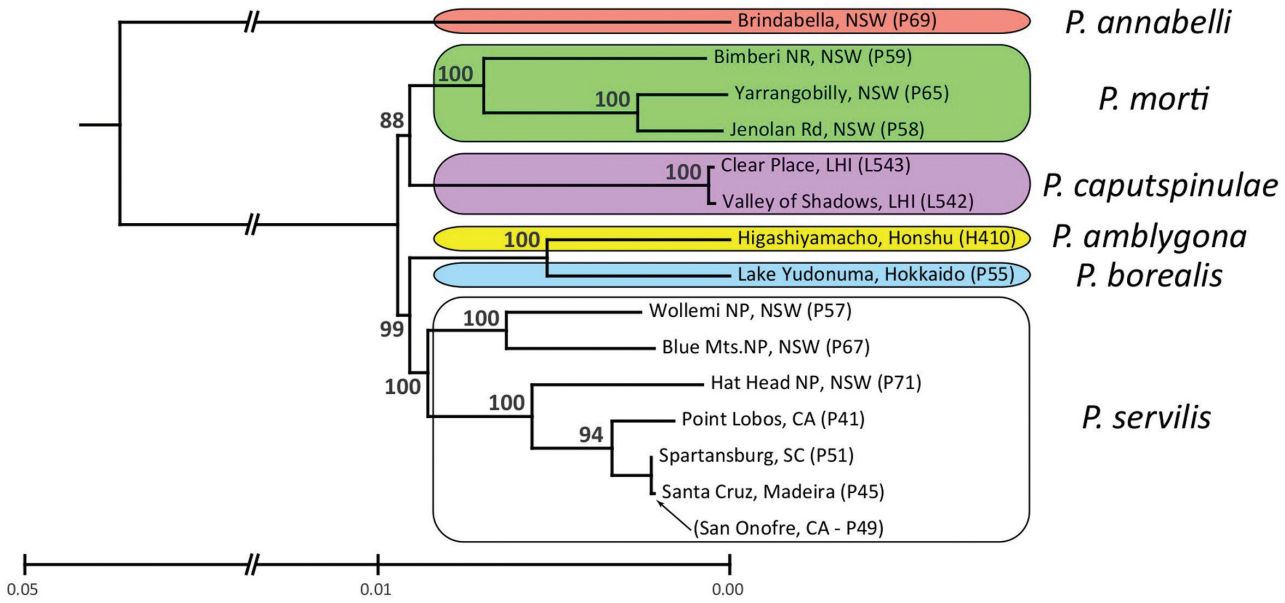

Figure 4. Maximum likelihood (ML) tree for ddRAD-Seq genomic analysis. Scale bars at the bottom represent maximum composite likelihood distances.

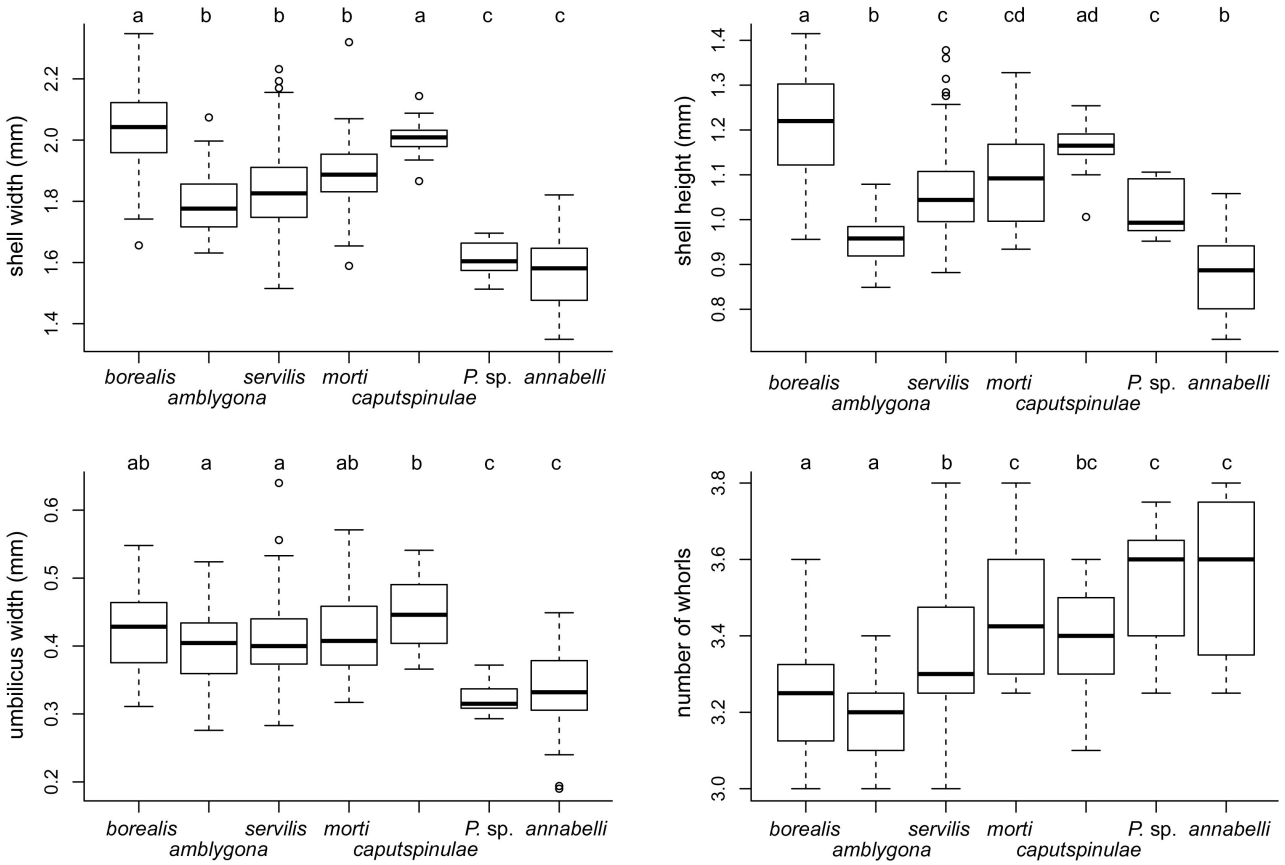

Figure 5. Box-plot comparisons of basic shell measurements among the seven genetically-validated species. The Kruskal–Wallis test demonstrated highly significant differences across all species ($P << .00001$) in all four comparisons. Post hoc identification of significant differences ($P = .05$) between individual box-plots within a panel were based on Dunn's test, with species sharing the same letter possessing insignificant differences.

The resultant library was then amplified for 10 PCR cycles, with final primer concentration being adjusted to 0.5 μM. Finally, the amplified sample was purified with 200–400 bp DNA fragments being collected using Pippin Prep (Sage Science, MA, USA). The DNA library was sent to BGI Japan (Hyogo) and sequenced using DNBseq-g400 with the paired-end 150-bp setting. The

Figure 6. Representative shell images for all genetically validated species. A, *Paralaoma borealis*, Yellow Post Fen, San Bernardino Co., California, 34.2230 N., 116.9410 W., JCN 19194, (P40); B, *Paralaoma amblygona*, Geibikei Gorge, Iwate Prefecture, Honshu, Japan, 38.9873 N., 141.2557 E., (P54); C, *Paralaoma servilis*, Rua da Riberia, Madeira, 32.693 N., 16.804 W., (P45); D, *Paralaoma morti*, Yarrangobilly Caves, Kosciuszko National Park, New South Wales, Australia, 35.725 S., 148.491 E., AM C.588490, (P65); E, *Paralaoma caputspinulae*, Valley of Shadows, Lord Howe Island, AM C.583303, (L542); F, *Paralaoma* sp. NZ, Lake Pukaki, Canterbury, South Island, New Zealand, 44.1754 S., 170.1645 E., NMNZ M.089606, (H376); G, *Paralaoma annabelli,* Magpie Flats, Bimberi Reserve, New South Wales, Australia, 35.617 S., 148.672 E., AM C.589836, (P60), note that the lower *P. annabelli* shell with frontal view is from the collection lot AM C.589837, representing a fully grown individual.

sequenced raw reads were then processed for *de novo* assembly using IPYRAD v.0.7.29 (Eaton and Overcast 2020). We specified a minimum coverage of eight (>50%) samples per locus, with strict filter adapters (filter_adapters = 2) to completely remove the Illumina adaptor sequences. Obtained SNPs were then used for ML reconstruction based on concatenated sequences

Table 2. Interquartile variation in (A) measured shell characteristics (B) and description of qualitative conchological features within and between *Paralaoma* species.

A. Shell measurements

Shell Feature	*P. amblygona* (*N* = 20)	*P. borealis* (*N* = 28)	*P. servilis* (*N* = 89)	*P. morti* *N* = 24)	*P. caputspinulae* (*N* = 19)	*P.* sp. NZ (*N* = 11)	*P. annabelli* (*N* = 19)
Height (mm)	0.9–1.0	1.1–1.2	1.0–1.1	1.0–1.2	1.1–1.2	1.0–1.1	0.8–0.9
Width (mm)	1.7–1.9	2.0–2.1	1.8–1.9	1.8–1.9	2.0–2.1	1.6–1.7	1.5–1.7
Aperture Height (mm)	0.67–0.72	0.81–0.90	0.72–0.80	0.72–0.82	0.82–0.85	0.62–0.66	0.52–0.59
Aperture Width (mm)	0.66–0.74	0.83–0.93	0.72–0.80	0.70–0.77	0.80–0.83	0.64–0.70	0.60–0.68
Umbilicus Width (mm)	0.36–0.43	0.38–0.46	0.37–0.44	0.37–0.45	0.41–0.49	0.31–0.34	0.31–0.38
Whorl Count	3.1–3.25	3.1–3.3	3.25–3.5	3.3–3.6	3.3–3.5	3.4–3.7	3.4–3.8
Shell Height/Width	0.52–0.54	0.57–0.62	0.56–0.60	0.56–0.61	0.56–0.59	0.62–0.65	0.53–0.59
Aperture Height/Width	0.93–1.01	0.95–0.99	0.95–1.05	1.00–1.06	1.00–1.05	0.93–0.99	0.84–0.92
Umbilicus/Shell Width	0.21–0.24	0.19–0.22	0.22–0.24	0.20–0.23	0.21–0.24	0.19–0.21	0.20–0.23
Coiling Ratio (mm/rev)	0.56–0.59	0.60–0.65	0.52–0.57	0.50–0.58	0.58–0.62	0.44–0.48	0.42–0.47

B. Qualitative shell characters

Shell Feature	*P. amblygona*	*P. borealis*	*P. servilis*	*P. morti*	*P. caputspinulae*	*P.* sp. NZ	*P. annabelli*
Margin shape	Shouldered	Weakly shouldered	Weakly shouldered	Weakly shouldered	Evenly rounded	Evenly rounded	Shouldered
Protochonch lirae							
Strength	Weak	Absent to weak	Absent to weak	Strong	Weak	Strong	Moderate
Number	~10–12	~15–20	~10–12	~10–12	~12–16	~6–8	~10–12
Major ribs							
Height	High	Low	Low/readily wear off	High	Low/readily wear off	High	Very high
Number per final ¼ revolution of Body Whorl	~12	~12	~12	~8	~12	~12	~6
Aperture shape	Elliptical	Elliptical	Elliptical	Elliptical	Round	Round	Narrowly elliptical

using IQ-TREE v.2.2.0 (Minh *et al.* 2020). The TVM+F+I+I+R7 nucleotide substitution model was selected using ModelFinder Plus (Kalyaanamoorthy *et al.* 2017). ML tree topologies were evaluated using ultrafast bootstrapping (Hoang *et al.* 2018) with 1000 replicates.

Traditional and geometric morphometric conchometrics

Shell morphospace variation between genetically verified species was investigated using both traditional univariate and geometric multivariate morphometrics (Karanovic *et al.* 2016, Horsáková *et al.* 2022). Analyses were limited to adult or near-adult shells (≥3 whorls) from genetically verified populations. The assumption that only a single genetically verified species was present per site appears valid in all of our analysed populations. Our final specimen set consisted of 20 *Punctum amblygonum* individuals from two populations, 19 *Paralaoma annabelli* individuals from three populations, 28 *Punctum boreale* individuals from six populations, 19 *Paralaoma caputspinulae* from four populations, 24 *Paralaoma morti* from three populations, 84 *Paralaoma servilis* from 14 populations, and 11 *Paralaoma* sp. NZ from one population. We also derived data from images or drawings of type specimens for *Punctum* (*Toltecia*) *boreale* Pilsbry and Hirase, 1905 (ANSP 90230—lectotype, online image), *Helix* (*Patula*) *amblygona* Reinhardt 1877 (Reinhardt 1877: holotype, drawing), and *Helix servilis* Shuttleworth, 1852 (Neubert *et al.* 2015: syntype—ZMZ 503343, image). In addition, measurements were made of one *P. morti* syntype (AM C.31181) and four *Paralaoma raoulensis* Iredale, 1913 paralectotypes from Raoul Island (AM C.30249). In total, 218 shells were measured.

The lectotype of *Helix caputspinulae* (NHMUK 1962724) was too damaged to be useful for conchometric analysis (see: Brook and Ablett 2019: pl. 8, fig. A), but we were able to assess some of its qualitative shell characters, such as shell margin shape, major rib development, relative size, and whorl expansion rate. In these it is indistinguishable from shells in populations spanning the New Zealand archipelago from the Three Kings Islands to Rakiura/Stewart Island and Chatham Island. We also did not measure specimens from the 1000+ shell-type lot of *Punctum conspectum alleni* Pilsbry, 1919 (ANSP 456955) because no holotype was officially designated. However, an illustrated shell from this lot in Pilsbry (1948: fig. 357c) agrees well with our measured material.

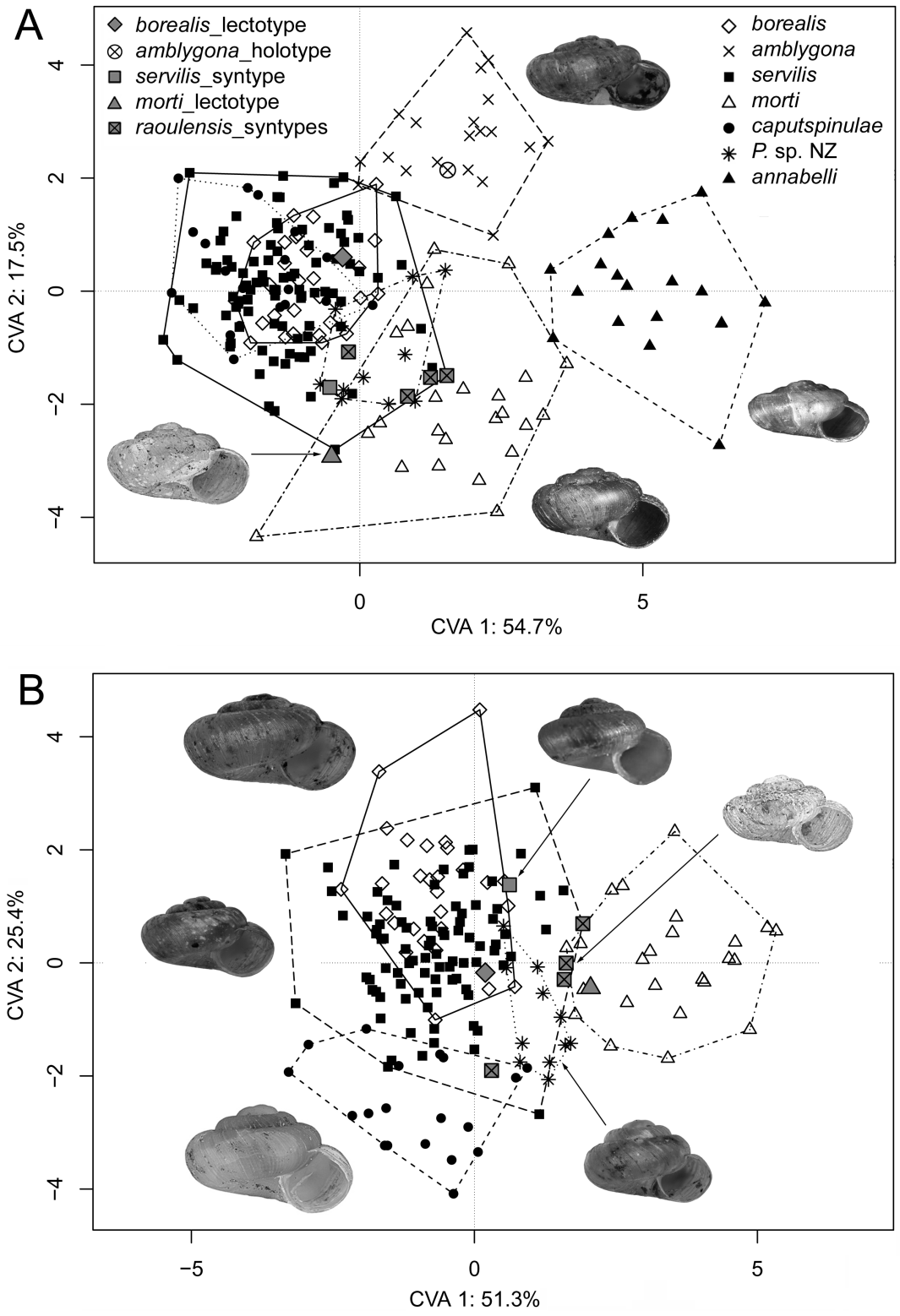

Figure 7. Location of each measured specimen along Axes 1 and 2 of the CVA based on 17 shell landmarks, including all type specimens (A) and after excluding *P. amblygona* and *P. annabelli* species to allow analysis differentiate highly overlapping taxa (B). Note that types for *P. amblygona* and *P. borealis* are not shown due to low quality of the drawing or image, while *P. caputspinulae* type is not shown due to immature and damaged shell.

Each shell was imaged from top, bottom, and front using an Olympus SZX7 microscope with Olympus C-7070 Wide Zoom camera and QuickPHOTO MICRO software. Deep focus was accomplished by assembling four to nine sequential stacked images. Shell width and height, aperture width and height, and umbilicus width were then determined (Fig. 2). Whorl number

Table 3. Classification accuracy of *Paralaoma* individuals identified via *ELAV* phylogeny vs. CVA based on Procrustes shape coordinates of 17 landmarks in shell apertural view. Rows represent specimen IDs based on genetically verified diagnostic traits. Columns represent assignments based on CVA landmark analysis. Across the entire suite of seven measured taxa (A), classification accuracy was 87.6%. When CVA was repeated on the five taxa most similar to *P. servilis* (B), classification accuracy was 84.8%

A. All indiv.	***P. amblygona***	***P. borealis***	***P. servilis***	***P. morti***	***P. caputspinulae***	***P.* sp. NZ**	***P. annabelli***
P. amblygona	21	0	0	0	0	0	0
P. borealis	0	20	8	0	1	0	0
P. servilis	0	6	82	2	3	1	0
P. morti	2	0	1	22	0	0	0
P. caputspinulae	0	0	3	0	16	0	0
P. sp. NZ	0	0	0	0	0	11	0
P. annabelli	0	0	0	0	0	0	19
B. Reduced		***P. borealis***	***P. servilis***	***P. morti***	***P. caputspinulae***	***P.* sp. NZ**	
P. borealis		21	8	0	0	0	
P. servilis		7	81	1	4	1	
P. morti		0	1	24	0	0	
P. caputspinulae		0	3	0	16	0	
P. sp. NZ		1	1	0	0	9	

Table 4. Vectors of maximum correlation and total explained variance for specimen shell characteristics vs location within the first three axes of the CVA based on 17 landmarks. *P*-values are based on a Monte Carlo permutation test with 1999 runs.

A. All individuals	**CVA 1**	**CVA 2**	**CVA 3**	**r^2 (%)**	***P***
Shell height	–0.671	–0.704	0.235	34.0	<.001
Shell width	–0.778	0.021	0.628	24.3	<.001
Shell height/Shell width	–0.185	–0.955	–0.233	50.5	<.001
Aperture height	–0.903	–0.124	0.411	50.4	<.001
Aperture width	–0.969	–0.248	0.023	28.1	<.001
Aperture height/Aperture width	–0.858	0.507	–0.084	38.1	<.001
Coiling ratio (mm/rev)	–0.468	0.341	0.815	19.8	<.001
Umbilicus width	–0.145	0.580	0.802	11.7	<.001
Umbilicus width/Shell width	–0.671	–0.704	0.235	34.0	<.001
B. Excluding *P. annabelli* and *P. amblygona*	**CVA 1**	**CVA 2**	**CVA 3**	**r^2 (%)**	***P***
Shell height	–0.119	–0.736	–0.667	3.4	.146
Shell width	–0.596	0.609	–0.523	6.4	.019
Shell height/Shell width	0.384	–0.917	–0.109	33.3	<.001
Aperture height	–0.909	0.404	–0.103	13.5	<.001
Aperture width	–0.921	–0.385	0.056	10.0	<.001
Aperture height/Aperture width	–0.975	0.175	0.140	16.7	<.001
Coiling ratio (mm/rev)	–0.391	0.873	–0.292	13.6	<.001
Umbilicus width	–0.284	0.953	–0.109	12.2	<.001
Umbilicus width/Shell width	–0.119	–0.736	–0.667	3.4	<.001

was recorded according to Cameron (2003). We also calculated ratios of shell height/shell width, umbilicus width/shell width, and aperture height/aperture width. Descriptive statistics for shell measurements are illustrated as box plots, with the significance of differences between taxa being estimated by the Kruskal–Wallis test with post hoc Dunn test.

Finally, the position of 17 shell landmarks (Fig. 2) was recorded. These were analysed via canonical variance analysis (CVA) in R 3.5.2 using the 'ADE4' (Dray and Dufour 2007), 'VEGAN' (Oksanen *et al.* 2017), and 'GEOMORPH' (Adams *et al.* 2021) packages. This direct ordination technique determines the three most important axes of variation in relative landmark position using genetic species' identification as the independent variable. Significance was estimated from 10 000 permutations of Mahalanobis and Euclidean distances using the 'MORPHO' package (Schlager 2017). Vectors of maximum correlation

within the 3D CVA ordination space were determined for the nine measured shell traits and calculated ratios using 4999 Monte Carlo permutations. The amount of overlap between each species in CVA space was also recorded.

Lastly, qualitative shell traits were noted and included margin shape, protoconch/teleoconch surface microsculpture, and the presence/arrangement/relative spacing of major growth ribs. Surface features were imaged using a Keyence VHX-5000 digital microscope with ZS-20 and ZS-200 objective lenses, and evaluated for all specimens used in morphometric analyses.

RESULTS

PCR amplicon phylogenetics

ELAV sequence was obtained from 44 individuals (Fig. 3), with the sequenced amplicon ranging from 688 to 690 bp. The outgroup *Miselaoma sinistra* individual possessed a 697-bp amplicon. All were placed into an 828-bp alignment, of which 130 bp were variable. ML and BI tree reconstructions both indicated that *Paralaoma annabelli* is quite distinct (ML and BI support values = 100). The remainder fell into five reciprocally monophyletic species-level clades with high support (ML = 81–100, BI = 99–100). On average 1.0–3.6 bp variability was noted within these clades. *Punctum conspectum alleni* is a member of the same highly supported species-level clade (81/100) as *Punctum boreale*: given that the name *boreale* has precedence, and that this entity requires transferring to *Paralaoma*, gender agreement requires change of the taxon name to *Paralaoma borealis*. Transfer to *Paralaoma* is also required for *Punctum amblygonum*, with the binomial changing to *Paralaoma amblygona*. From 6.7 to 10.5 bp differences were noted between *P. amblygona*/*P. borealis*/*P. caputspinulae*/*P. morti*/*P. servilis*, while 50–53 bp differences were noted between these and *P. annabelli*. *Miseolaoma sinistra* differed by 62.8–64.8 bp from all analysed *Paralaoma* taxa. Because of the distinctness between the six clades, in combination with their unique conchology (see below), we interpret all as being distinct biological species. *Paralaoma caputspinulae* also demonstrated a unique, highly supported (97–100) subclade limited to Lord Howe Island, which differed by 2–5 bp from New Zealand populations.

Amplified *COI* sequence was obtained from 47 samples (Fig. 3). The sequenced amplicon was 655 bp in length, with 185 variable base pairs. Both ML and BI tree reconstructions documented topological variation from *ELAV* and a considerably more complex evolutionary history. While *Paralaoma annabelli*, *P. amblygona*, and *P. borealis* all possessed single, highly supported (ML = 82–100; BI = 100 BI), reciprocally monophyletic clades, the other species exhibited multiple highly supported non-coalescing *COI* clades. *Paralaoma caputspinulae* demonstrated two separate highly supported clades, with Lord Howe Island material being sister to *P. servilis* (ML and BI = 100), whereas New Zealand material was sister to *P. morti* (ML = 99; BI = 100). *Paralaoma morti* also possessed two distinct clades: one being sister to New Zealand *P. caputspinulae* (ML = 81; BI = 98) and the other being sister to *P. borealis* (ML and BI = 100). Lastly, *P. servilis* possessed three distinct clades, one of which is sister to *P. caputspinulae* (ML = 63; BI = 73). The members of this clade are generally sourced from western North America, south-eastern USA, and Macaronesia. The other two *P. servilis* clades are sister to the *P. amblygona/borealis* clade. One (ML = 96; BI = 100) is limited to New South Wales, while the other (ML = 99/BI = 100) is limited to Macaronesia and France.

Base pair variation within the two Paralaoma morti clades ranged from 0 to 25, respectively. The *P. morti* specimen from Cooleman Caves (P59) possessed a long branch; while distinct mutations and/or indels can be present in cave-dwelling populations of widely distributed species (Salvador, unpublished data), this branch could also represent an undescribed new species. Outside of *P. morti*, average within-group variability ranged from 0.7 bp in *P. amblygona* to 18 bp in *P. servilis* clade 1. The number of variable bases between non-coalescing mitochondrial clades within a given species ranged from 31 to 42. On average, 24 base pairs varied between different species, with 52 bases separating *P. annabelli/Paralaoma* sp. NZ from the remaining *Paralaoma* taxa.

Additionally, two instances of possible mitochondrial introgression were noted with an individual from Washington USA (P52) having typical *P. servilis ELAV* sequence and shell features but *P. borealis COI* sequence, and one British Columbia individual (P28) having typical *P. borealis ELAV* sequence and shell features but *P. servilis COI*. Incomplete sorting can be discounted as the underlying mechanism given that *P. borealis* and *P. servilis* are not sister-species that have diverged on the North American Pacific Coast.

ddRAD phylogenetics

We analysed 41 750 SNPs distributed across 746 103 bp in 2867 loci from 14 specimens (Fig. 4). Raw sequences were deposited in the NCBI Sequence Read Archive (SAMN3369177-SAMN3369190). Generated phylogenetic trees showed strong support (100) and/or considerable genetic distance (0.5% of base pairs) between *Paralaoma amblygona*, *P. annabelli*, *P. borealis*, *P. caputspinulae*, *P. morti*, and *P. servilis*. Genetic distance between *P. annabelli* and the remaining species was approximately 5% of base pairs. The Cooleman Cave *P. morti* specimen again exhibited a long (>0.5%) branch from the other *P. morti*, suggesting that it could represent a distinct taxon. Additionally, ddRAD-Seq allowed for deeper node resolution at high support: *P. morti* and *P. caputspinulae* were shown to be sister (ML support = 88). *Paralaoma amblygona*, *P. borealis*, and *P servilis* (99) were found to be members of the same clade, with *P. amblygona* and *P. borealis* being sister (100). Considerable structure was noted within *P. servilis*, with the Wollemi and Blue Mountains National Park, New South Wales populations being clustered (100) but distinct from each other. The remaining subclade (100) included the Hat Head National Park, New South Wales population, which was more than 0.5% distinct from the remaining highly supported (94) subclade consisting of western USA, south-eastern USA, and Madeira populations. Within this subclade the Point Lobos State Natural Area population was distinct from South Carolina and Madeira populations. While the limited number of returned loci prevented inclusion of the San Onofre State Beach population into this clade, comparison of its available SNPs indicated that it was essentially identical.

Conchometrics

All six measured shell traits (height, width, aperture height, aperture width, umbilicus width, and whorl count) demonstrated

highly significant differences between the genetically demarcated species (Kruskal–Wallis $P << .000001$; Figs 5, 6). Shell width fell into three significant groups: *Paralaoma borealis* and *P. caputspinulae* possessed the largest shells with an interquartile range of 2.0–2.1 mm; *P. amblygona*, *P. morti*, and *P. servilis* with a range of 1.7–2.0 mm; and *P. annabelli* and *P.* sp. NZ with a range of 1.5–1.7 mm. Three significant groups were present in shell height: again *P. borealis* and *P. caputspinulae* were the largest with an interquartile range of 1.1–1.2 mm; *P. morti*, *P. servilis*, and *P.* sp. NZ ranged from 1.0 to 1.2 mm; with *P. amblygona* and *P. annabelli* both being <1 mm. Umbilicus width was divided into two groups with *P. borealis*, *P. amblygona*, *P. servilis*, *P. morti*, and *P. caputspinulae* having an interquatile range of 0.36–0.48 mm, and *P.* sp. NZ and *P. annabelli* ranging from 0.31 to 0.38 mm. Lastly, the number of whorls present in adult individuals represented three groups, ranging from 3.1 to 3.3 in *P. borealis* and *P. amblygona*, 3.25–3.5 in *P. servilis*, *P. morti*, and *P. caputspinulae*, and 3.3–3.8 in *P.* sp. NZ and *P. annabelli*. Because both aperture measurements were highly correlated with shell width ($P << .000001$; $r^2 = 0.786$ vs. aperture height and $r^2 = 0.753$ vs. aperture width) and demonstrated the same boxplot patterns, we use the shell width boxplot as a proxy for both.

Some of the ratios present between these variables appeared diagnostic (Fig. 6), with *Paralaoma* sp. NZ having the tallest shells (two-thirds of width), *P. annabelli* having the most compressed aperture (height < 0.6 of width), *P. borealis* and *P.* sp. NZ having the narrowest umbilicus as a proportion of shell width (~<1/5). *Paralaoma borealis* also had the greatest shell expansion rate (>0.6 mm shell diameter/whorl) with *P.* sp. NZ/*P. annabelli* having the least (<0.5 mm/whorl).

Diagnostic differences were noted in various qualitative shell traits (Table 2; Fig. 6): *Paralaoma caputspinulae* and *P.* sp. NZ were notable for their almost perfectly round margins and aperture shapes, while *P. amblygona*/*P. annabelli* were the most shouldered, especially on the lower surface. The number and strength of spiral lirae on the protochonch also appeared diagnostic, as was the height and spacing of major ribs on the body whorl. Additionally, the protochonch of *P. caputspinulae* is 15%–30% smaller than all other analysed species (save *P.* sp. NZ), which is remarkable given its large adult size.

Lastly, CVA of shell landmarks illustrates considerable segregation of *P. amblygona*, *P. morti*, and *P. annabelli* in morphospace (Fig. 7A). Because of their difference, the remaining taxa were compressed into a similar location along CVA Axes 1 and 2. However, overall misclassification rate was only 12% due to distinction in these taxa along unplotted CVA Axis 3 (Table 3). When *P. annabelli* and *P. amblygona* (the most divergent taxa) were excluded, and CVA repeated on the remainder, greater differentiation was seen among *P. borealis*, *P. caputspinulae*, *P. morti*, *P.* sp. NZ, and *P. servilis* (Fig. 7B). While considerable overlap was still noted between *P. borealis*, *P. caputspinulae*, and *P. servilis*, the misclassification rate was only 15%, again due to segregation along the unplotted third CVA axis. In addition, qualitative features not included in landmark analysis (such as protochonch lirae number/strength, major rib architecture, body whorl shape) allow for accurate identification of individuals possessing indeterminate landmark positions. In the CVA, the type specimens of *P. amblygona*, *P. borealis*, *P. morti*, and *P. servilis* all fell within the polygons defining their respective species groups. The four paralectotypes of *P. raoulensis* possessed landmarks consistent with placement in *P. servilis* but, given the observed overlap between *P. servilis* and its nearest neighbours, and the fact that their qualitative features were not assessed, we cannot definitively state whether *raoulensis* is a junior synonym of *servilis* or a separate species endemic to the Kermadec Islands. We can say, however, that the genus name *Paralaoma* can be applied to all other members of the group.

Five of the measured shell attributes, along with four of their calculated ratios, were found to significantly ($P <.001$) co-vary with the three CVA axes when all seven taxa were included (Table 4A). Shell height, aperture height, aperture width, shell height/width ratio, and umbilicus width/shell width ratio tended to increase towards the lower left-hand corner. Shell width tended to increase to the left side of CVA Axis 1. Aperture height/width, coiling ratio, and umbilicus width tended to increase to the upper left of the diagram. When CVA was rerun after exclusion of *P. amblygona* and *P. annabelli* (Table 4B), seven shell attributes were found to be highly significantly correlated ($P < .001$) with the CVA diagram. Shell width was only moderately correlated ($P = .019$), while shell height was not significantly correlated ($P = .146$). Shell width, aperture height, aperture height/width ratio, coiling ratio, and umbilicus width tended to increase towards the upper left of the diagram, while aperture width and umbilicus/shell width tended to increase towards the lower left. Shell height/width ratio tended to increase towards the lower right.

DISCUSSION

Rigorous hypothesis testing across multiple lines of evidence demonstrates that traditional classification of the *Paralaoma servilis* group obscured a more complex biological reality. While some prior taxonomic acts were validated (e.g. *Punctum conspectum* being a junior synonym of *P. servilis*; *P. annabelli* and *P. morti* being treated as distinct species), considerable issues remained. For example, *P. caputspinulae* had been lumped into *P. servilis*, but our analyses indicate that it is a distinct species ranging across New Zealand and Lord Howe Island with populations on the latter forming a marked subclade possessing unique mtDNA. This species has been observed in Holocene fossil assemblages antecedent to human arrival on both landmasses (Brook *et al.* 2020; F. Brook, unpublished data). Our findings also show that both *Punctum amblygonum* and *Punctum boreale* are members of the *P. servilis* group. In addition, *Punctum conspectum alleni* was found to be conspecific with *P. borealis*. Images of type material for *Punctum* (*Toletecia*) *rota* Pilsbry and Hirase, 1904 from the Academy of Natural Sciences of Philadelphia website (http://clade.ansp.org/malacology/collections/details.php?mode=details&catalognumber=87930) suggest that this taxon is also probably attributable to *Paralaoma*. Careful re-evaluation of the generic placement of East Asian *Punctum* species is thus in order.

A reason for the inaccuracy of traditional taxonomy in this group is that previous diagnoses were based on plastic shell characters. This contributed to the convoluted taxonomic history of this complex. Although all *Paralaoma* species examined here have broadly similar shell morphologies, consistent diagnostic

differences do exist between them and include shell size, coiling ratio, umbilicus to shell width ratio, the degree of flattening of the shell margin, and the nature of spiral lirae on the protoconch and major ribs on the teleoconch (Table 2). These latter features have previously been considered important in both genus- and species-level diagnoses within the group (e.g. Pilsbry 1948, Hylton Scott 1957, Solem 1983, Marshall and Worthy 2017). In general terms, the diagnostic shell traits for the taxa considered here are:

Paralaoma annabelli has a relatively tightly-coiled shell ≤1.7 mm in diameter, with shouldered, sharply-rounded whorls, high, widely-spaced teleoconch ribs, and a protoconch with ~10–12 spiral lirae.

Paralaoma amblygona has a relatively loosely-coiled shell ≥1.7 mm in diameter, with shouldered, sharply-rounded whorls, moderately high teleoconch ribs, and a protoconch with ~10–12 weak spiral lirae.

Paralaoma borealis has a relatively loosely-coiled shell ≥1.7 mm in diameter, with weakly shouldered whorls and a protoconch with 15+ weak spiral lirae. This species demonstrates clinal variation across its range with umbilicus width becoming proportionately narrower, shell height lower, and teleoconch ribs taller in Hokkaido populations. The name *P. borealis alleni* is available to designate North American populations possessing taller, more weakly ribbed shells.

Paralaoma caputspinulae is distinguished by its relatively large shell, with evenly rounded whorls, weak and irregularly-spaced teleoconch ribs, and small protoconch with ~15 strong densely spaced spiral lirae.

Paralaoma sp. NZ has a relatively tightly-coiled shell ≤1.7 mm in diameter, with high spire, evenly rounded whorls, and a protoconch with ~6–8 widely spaced spiral lirae.

Paralaoma morti has a relatively loosely-coiled shell ~1.8–1.9 mm diameter, with weakly shouldered whorls, moderately high teleoconch ribs, and a protoconch with ~10–12 spiral lirae.

Paralaoma servilis is very similar to *P. morti*, but differs in having much weaker sculpture on the teleoconch and protoconch and a relatively wider aperture.

It seems likely that *Paralaoma* will prove to be even more diverse than indicated here. First, the presence of long branch-tip SE Australian individuals within both *P. morti* and *P. servilis* may be indicative of other, as yet unrecognized, species. Second, published illustrations appear to indicate that local native species of this genus are present elsewhere in Asia and the Pacific islands. For instance, the *P.* '*servilis*' illustrated from a remote Nepalese forest (Gittenberger *et al.* 2020), does not fall within our concept of *P. servilis* because of its strong protoconch lirae, and moderately tall and strong teleoconch ribs. Instead, it looks closer to *P. morti*, and may well represent an undescribed native taxon. Similarly, the Christensen *et al.* (2012) illustration of an O'ahu, Hawaiian Islands shell also does not fall into our concept of *P. servilis*, given its tall, loosely-coiled shell, with very large aperture and narrow umbilicus. While this shell is reminiscent of *P. borealis*, we again suspect that it could represent yet another species-level taxon. We, therefore, recommend that any putative *P. servilis* population from western, southern, and south-eastern Asia and adjacent Oceania (e.g. Indonesia, Nurinsiyah and Hausdorf 2019; Georgia, Pokryszko *et al.* 2011) have their genetics and conchology carefully scrutinized.

Our ability to document the subtle but consistent differences between these species was only possible by limiting conchological comparisons to lots that had first been sorted into their respective nDNA genetic groups. Without this, diagnostic morphological traits would have been lost within the sea of total variability. We also note that arranging shells by their mtDNA groups would have failed due to common species-scale polyphyly. Once robust diagnostic traits were identified, however, it was possible to accurately re-identify lots, including those containing only empty shells. From this we determined available *nomina* through observations of type material. While it has become common to juxtapose DNA signal and conchology, and consider which is more trustworthy (e.g. Páll-Gergely 2017), we instead argue—as have many others (e.g. Wheeler 2023)—that documentation of morphological variability within populations is only made possible through genetic control, thereby achieving greater clarity in taxonomic decision-making.

Finally, these analyses help suggest the possible historical biogeography of invasive *Paralaoma servilis* populations. We first note that these appear restricted to a single subclade. This is not unique and has been seen in other widespread invasive species [e.g. *Gyraulus parvus* (Say, 1817); Lorencová *et al.* 2021]. We suggest three potential hypotheses regarding the origin of this invasive subclade:

First, given that *Paralaoma servilis* appears most genetically diverse within SE Australia, it is possible that the invasive clade originated there but has simply been overlooked. In this scenario, native populations were accidentally picked up by early European explorers and carried separately to the eastern Atlantic/Mediterranean and North American Pacific coasts. The main supporting argument for this is the distinct mtDNA clade limited to Europe/Macronesian Islands, where it coexists with the other *P. servilis* mtDNA clade, suggesting the presence of more than one founding population. The main supporting argument against this hypothesis is that *P. servilis* was apparently well established in Madeira (the type locality for the first *nomena* associated with this taxon) by 1831, implying initial colonization on or before the early 1800s. Given that European contact with eastern Australia did not happen until 1770, there seems to be limited time for this scenario to have played out. Even so, species can naturalize and spread within a single decade (e.g. Rosa *et al.* 2022). The transport of *Eucalyptus* to coastal California cannot explain the initial colonization of *P. servilis* there, however, because initial transportation from eastern Australia did not happen until 1853 (Weir 1957, Groenendaal 1983), at least two decades after the North American Pacific Coast race had colonized Madeira.

Second, it is possible that by some unknown vector, and at some unknown time, *Paralaoma servilis* was able to cross the Pacific Ocean unaided by humans and naturally establish populations on the North American coast, after which they diverged into multiple races with one being highly invasive. While appearing exceedingly unlikely, given the lack of any other known natural species-scale trans-Pacific disjunctions or jump-dispersal

vectors [but see Holstein *et al.* (2016) for pan-Pacific disjunctions within the plant family Boraginaceae and Saito *et al.* (2023) for latitudinal dispersal of freshwater snail species by birds across the western Pacific], this option cannot be totally ruled out given the presence of gene-pool diversification within coastal California populations and the existence of multiple cases of apparent mitochondrial introgression between *P. servilis* and *P. borealis*. Such interactions should be rare given how little their current ranges overlap.

A third option is that the direct ancestor to the invasive *Paralaoma servilis* race is indigenous to areas north of Australia. These areas came into contact with European traders much earlier: by 1565 the Spanish had developed a trans-Pacific trading route that started at Acapulco, Mexico and carried New World gold and silver to the Philippines and China in return for spices, silks, and porcelains. Returning ships typically encountered the North American mainland around Cape Mendocino and then used the California current to return to their starting point. Beginning in 1587, their cargo was enlarged to include Filipino slaves, prisoners, and crew with encampments occurring at Morro Bay (Mercene 2007). Transporting and feeding human cargo would have involved movement of considerably more biological material, increasing the chance that a hitchhiking snail was brought along. Given that the invasive *P. servilis* clade has yet to be observed within the south-west Pacific Rim, it is also possible that it could have evolved in coastal California from a severely bottlenecked founder population. Following establishment across low elevations in California, this race could have then been carried by the Spanish across its global trade network.

CONCLUSION

Paralaoma servilis is not a single tramp species of New Zealand or Australian origin as suggested by traditional taxonomy, but rather represents several distinct native species that extend along the Pacific Rim to at least the SW USA. Populations currently identified as this species from western, southern, and south-east Asia and associated archipelagos should be genetically and conchologically investigated to see if they actually represent native taxa. While the centre of *Paralaoma* biodiversity appears to be in eastern Australia, the single highly invasive subclade of *P. servilis* appears to have had long residence along the USA/Mexico Pacific coast. Although the origin of this population cannot be conclusively determined, it seems possible that its ancestors were brought to the North American west coast via east-Asian Spanish trade in the late 1500s. It was this race that then expanded across low elevations in California and western Mexico, from where it was carried by international commerce to the global reach of temperate to tropical habitats.

This work is as reminder that biodiversity statistics and conservation strategies are only as reliable as the taxonomy upon which they are based. Here, an overly broad concept of *Paralaoma servilis* has resulted in a number of native, distinct species being perceived as invasive pests within their native ranges. Thus, rather than being recognized as contributors to their local native biodiversity, they were written off as examples of anthropogenic homogenization. And at the same time, the habitats supporting them were downrated in their conservation importance (NatureServe 2024). Empirical vetting of taxonomic concepts is thus an essential prerequisite to accurate biodiversity and conservation assessments.

ACKNOWLEDGEMENTS

We thank Brian Coles for providing analyzed French coast and António Frias Martins for Azorean material. We thank the Museum of New Zealand Te Papa Tongarewa for granting access to their DNA lab for the part of this study done in Aotearoa New Zealand, and to Lara Shepherd for help with lab work.

FUNDING

This study was partially funded by a research grant (Hutton Fund) to RBS from the Royal Society Te Apārangi, Aotearoa New Zealand, the Wildlife and Habitat Bushfire Recovery Program Grants GA2000821, GA2000869, and GA2000885 from the Department of Agriculture, Water and the Environment, Australia, and Czech Science Foundation Grant 22-23005S.

CONFLICT OF INTEREST

None declared

DATA AVAILABILITY

The DNA sequences underlying this study are available in NCBI GenBank and Sequence Read Archive as per above text and tables. Specimens are deposited in: Australian Museum (Syndey, Australia), Museum of New Zealand Te Papa Tongarewa (Wellington, New Zealand); University of Otago (Dunedin, New Zealand); Department of Botany and Zoology, Masaryk University (Brno, Czech Republic).

REFERENCES

Adams DC, Collyer ML, Kaliontzopoulou A *et al. Geomorph: Software for Geometric Morphometric Analyses. R Package v.3.3.2*, 2021.

Boxnick A, Apio A, Wronski T *et al.* Diversity patterns of the terrestrial snail fauna of Nyungwe Forest National Park (Rwanda), a Pleistocene refugium in the heart of Africa. *Biological Journal of the Linnean Society* 2015;**114**:363–75. https://doi.org/10.1111/bij.12418

Brook FJ, Ablett JD. Type material of land snails (Mollusca: Gastropoda) described from New Zealand by taxonomists in Europe and North America between 1830 and 1934, and the history of research on the New Zealand land snail fauna from 1824 to 1917. *Zootaxa* 2019;**4697**:1–117.

Brook FJ, Kennedy M, King TM *et al.* Catalogue of New Zealand land, freshwater and estuarine molluscan taxa named by Frederick Wollaston Hutton between 1879 and 1904. *Zootaxa* 2020;**4865**:1–73.

Cameron R. *Land Snails in the British Isles.* Shropshire: Field Studies Council, 2003.

Christensen CC, Yeung NW, Hayes KA. First records of *Paralaoma servilis* (Shuttleworth, 1852) (Gastropoda: Pulmonata: Punctidae) in the Hawaiian Islands. *Bishop Museum Occasional Papers* 2012;**112**:3–7.

Conix S. Taxonomy and conservation science: interdependent and value-laden. *History and Philosophy of the Life Sciences* 2019;**41**:15. https://doi.org/10.1007/s40656-019-0252-3

Costello MJ, Vanhoorne B, Appeltans W. Conservation of biodiversity through taxonomy, data publication, and collaborative infrastructures. *Conservation Biology* 2015;**29**:1094–9.

Darriba D, Taboada GL, Doallo R *et al.* jModelTest 2: more models, new heuristics and parallel computing. *Nature Methods* 2012;**9**:772. https://doi.org/10.1038/nmeth.2109

Dillon TJ, Metcalf AL. Altitudinal distribution of land snails in some montane canyons in New Mexico. In: Metcalf AE, Smartt RA (eds), Land Snails of New Mexico. *New Mexico Museum of Natural History and Science, Bulletin* 1997;**10**:109–27.

Dray S, Dufour A. The ade4 package: implementing the duality diagram for ecologists. *Journal of Statistical Software* 2007;**22**:1–20.

Drummond AJ, Rambaut A. BEAST: Bayesian evolutionary analysis by sampling trees. *BMC Evolutionary Biology* 2007;**7**:214.

Eaton DAR, Overcast I. ipyrad: interactive assembly and analysis of RADseq datasets. *Bioinformatics* 2020;**36**:2592–4. https://doi.org/10.1093/bioinformatics/btz966

Felsenstein J. Confidence limits on phylogenies: an approach using the bootstrap. *Evolution* 1985;**39**:783–91. https://doi.org/10.1111/j.1558-5646.1985.tb00420.x

Foon JK, Green PT, Köhler F. Delineating *Paralaoma annabelli*, a minute land snail impacted by the 2019–2020 wildfires in Australia. *Records of the Australian Museum* 2023;**75**:51–64.

Gittenberger E, Budha PB, Bank RA. Amazing *Paralaoma servilis* (Gastropoda, Pulmonata, Punctidae) in Nepal. *Basteria* 2020;**84**:76–82.

Groenendaal GM. *Part 1. History of Eucalypts in California. General Technical Report of the Pacific Southwest Forest and Range Experimental Station 69*. Berkeley: US Forest Service, 1983.

Hausdorf B. Introduced land snails and slugs in Columbia. *Journal of Molluscan Studies* 2001;**68**:127–31.

Hausdorf B. Distribution patterns of established alien land snail species in the Western Palaearctic Region. *NeoBiota* 2023;**81**:1–32. https://doi.org/10.3897/neobiota.81.96360

Hoang DT, Chernomor O, Von Haeseler A *et al.* UFBoot2: improving the ultrafast bootstrap approximation. *Molecular Biology and Evolution* 2018;**35**:518–22.

Holstein N, Chacón J, Otero A *et al.* Towards a monophyletic *Omphalodes*—or an expansion of the North American *Mimophytum*. *Phytotaxa* 2016;**288**:131–44.

Horsáková V, Líznarová E, Razkin O *et al.* Deciphering the 'cryptic' nature of European rock-dwelling *Pyramidula* snails (Gastropoda: Stylommatophora). *Contributions to Zoology* 2022;**91**:233–60. https://doi.org/10.1163/18759866-bja10032

Huelsenbeck JP, Ronquist F. MRBAYES: Bayesian inference of phylogenetic trees. *Bioinformatics* 2001;**17**:754–5. https://doi.org/10.1093/bioinformatics/17.8.754

Hylton Scott MI. Endodontideos neotropicales I. (Moll. Pulm.). *Neotropica* 1957;**3**:7–16.

Kalyaanamoorthy S, Minh BQ, Wong TKF *et al.* ModelFinder: fast model selection for accurate phylogenetic estimates. *Nature Methods* 2017;**14**:587–9. https://doi.org/10.1038/nmeth.4285

Karanovic T, Djurakic M, Eberhard SM. Cryptic species or inadequate taxonomy? Implementation of 2D geometric morphometrics based on integumental organs as landmarks for delimitation and description of copepod taxa. *Systematic Biology* 2016;**65**:304–27.

Katoh K, Toh H. Improved accuracy of multiple ncRNA alignment by incorporating structural information into a MAFFT-based framework. *BMC Bioinformatics* 2008;**9**:1–13.

Lorencová E, Beran L, Nováková M *et al.* Invasion at the population level: a story of the freshwater snails *Gyraulus parvus* (Say, 1817) and *G. laevis* (Alder, 1838). *Hydrobiologia* 2021;**848**:4661–71. https://doi.org/10.1007/s10750-021-04668-w

Marshall BA, Worthy TH. Miocene land snails (Mollusca: Gastropoda: Pulmonata) from palaeolake Manuherikia, southern New Zealand. *Journal of the Royal Society of New Zealand* 2017;**47**:294–318. https://doi.org/10.1080/03036758.2017.1287101

Martínez-Ortí A, Gómez-Moliner BJ, Prieto CE. El género *Pyramidula* Fitzinger 1833 (Gastropoda, Pulmonata) en la Península Ibérica. *Iberus* 2007;**25**:77–87.

Mercene FL. *Manila Men in the New World: Filipino Migration to Mexico and the Americas from the Sixteenth Century*. Manila: University of the Philippines Press, 2007.

Metcalf AL. Land snails of New Mexico from an historical zoogeographic point of view. In: Metcalf AE, Smartt RA (eds), Land Snails of New Mexico. *New Mexico Museum of Natural History and Science, Bulletin* 1997;**10**:71–108.

Minh BQ, Schmidt HA, Chernomor O *et al.* IQ-TREE 2: new models and efficient methods for phylogenetic inference in the genomic era. *Molecular Biology and Evolution* 2020;**37**:1530–4. https://doi.org/10.1093/molbev/msaa015

NatureServe. *NatureServe Conservation Status Assessments: Rank Calculator v.3.185*. http://connect.natureserve.org/publications/StatusAssess_Rank Calculator (1 June 2024, date last accessed).

Nekola JC, Horsák M. The impact of statistically unchallenged taxonomic concepts on ecological assemblages across multiple spatial scales. *Ecography* 2022;**2022**:e06063.

Nekola JC, Chiba S, Coles BF *et al.* A phylogenetic overview of the genus *Vertigo* O. F. Müller, 1773 (Gastropoda: Pulmonata: Pupillidae: Vertigininae). *Malacologia* 2018;**62**:21–161. https://doi.org/10.4002/040.062.0104

Nekola JC, Nováková M, Horsák M *et al. ELAV* Intron 8: a single-copy sequence marker for shallow to deep phylogeny in *Eupulmonata* Hasprunar & Huber, 1990 and *Hygrophila* Férussac, 1822 (Gastropoda: Mollusca). *Organisms, Diversity & Evolution* 2023;**23**:621–9. https://doi.org/10.1007/s13127-022-00587-3

Neubert E, Amr ZS, Waitzbauer W *et al.* Annotated checklist of the terrestrial gastropods of Jordan. *Archiv für Molluskenkunde* 2015;**144**:169–238.

Nurinsiyah AS, Hausdorf B. Listing, impact assessment and prioritization of introduced land snail and slug species in Indonesia. *Journal of Molluscan Studies* 2019;**85**:92–102. https://doi.org/10.1093/mollus/eyy062

Oksanen J, Blanchet FG, Friendly M *et al. vegan: Community Ecology Package. R v.2.4-3*, 2017. https://CRAN.R-project.org/package=vegan

Páll-Gergely B. Should we describe genera without molecular phylogenies? *Zootaxa* 2017;**4232**:593–6.

Peterson BK, Weber JN, Kay EH *et al.* Double digest RADseq: an inexpensive method for De Novo SNP discovery and genotyping in model and non-model species. *PLoS One* 2012;**7**:e37135. https://doi.org/10.1371/journal.pone.0037135

Pilsbry HA. Land Mollusca of North America (north of Mexico). *Academy of Natural Sciences of Philadelphia Monograph 3* 1948a;**2**.

Pilsbry HA. *Land Mollusca of North America (North of Mexico). Vol. 2, Part 2.* Philadelphia: The Academy of Natural Sciences of Philadelphia, 1948.

Pokryszko BM. On aphally in the Vertiginidae (Gastropoda: Pulmonata: Orthurethra). *Journal of Conchology* 1987;**32**:365–75.

Pokryszko BM, Cameron RAD, Mumladze L *et al.* Forest snail faunas from Georgian Transcaucasia: patterns of diversity in a Pleistocene refugium. *Biological Journal of the Linnean Society* 2011;**102**:239–50. https://doi.org/10.1111/j.1095-8312.2010.01575.x

Price GJ, Webb GE. Late Pleistocene sedimentology, taphonomy and megafauna extinction on the Darling Downs, southeastern Queensland. *Australian Journal of Earth Sciences* 2006;**53**:947–70. https://doi.org/10.1080/08120090600880842

Reinhardt O. Diagnosen japanischer Landschnecken. *Jahrbücher der Deutschen Malakozoologischen Gesellschaft* 1877;**4**:320–5.

Rosa RM, Salvador RB, Teixeira L *et al.* The rapid expansion of the jumping snail *Ovachlamys fulgens* in Brazil. *Diversity* 2022;**14**:815. https://doi.org/10.3390/d14100815

Rosenberg G, Muratov IV. Status report on the terrestrial mollusca of Jamaica. *Proceedings of the Academy of Natural Sciences of Philadelphia* 2005;**155**:117–61. https://doi.org/10.1635/i0097-3157-155-1-117.1

Roth B. Notes on three European land mollusks introduced to California. *Bulletin of the Southern California Academy of Sciences* 1986;**85**:22–8.

Rumi A, Sánchez J, Ferrando NS. *Theba pisana* (Müller, 1774) (Gastropoda, Helicidae) and other alien land mollusc species in Argentina. *Biological Invasions* 2010;**12**:2985–90.

Saito T, Tatani M, Odaya Y *et al.* Direct evidence for intercontinental dispersal of a snail via a bird. *Ecography* 2023;**2023**:e06771.

Schlager S. Morpho and Rvcg—shape analysis in R. In: Zheng G, Li S, Szekely G (eds), *Statistical Shape and Deformation Analysis*. New York: Academic Press, 2017, 217–56.

Schmid G. Der Bambus-Tick oder *Paralaoma servilis*, die Gerippte Punktschnecke. In: Falkner M, Groch K, Speight MCD (eds), *Collectanea Malacologica.* Harxheim, Germany: ConchBooks, 2002, 377–401.

Schütt H. Die Türkischen Landschnecken 1758–2000. 3. *Auflage, Acta Biologica Benrodis* 2001;**Supplement 4**:1–549.

Solem A. *Endodontoid Land Snails from Pacific Islands (Mollusca: Pulmonata: Sigmurethra). Part 2: Families Punctidae and Charopidae: Zoogeography*. Chicago, Field Museum of Natural History, 1983.

Stamatakis A. RAxML version 8: A tool for phylogenetic analysis and post-analysis of large phylogenies. *Bioinformatics* 2014;**30**:1312–3. https://doi.org/10.1093/bioinformatics/btu033

Steury BW, Pearce TA. Land snails and slugs (Gastropoda: Caenogastropoda and Pulmonata) of two national parks along the Potomac River near Washington, District of Columbia. *Banisteria* 2014;**43**:3–20.

Virgillito M, Miquel SE. New records of exotic land snails and slugs in Argentina. *Revista del Museo Argentino de Ciencias Naturales* 2013;**15**:295–303. https://doi.org/10.22179/revmacn.15.186

Weir DA. *That Fabulous Captain Waterman.* New York: Comet Press Books, 1957.

Welter-Schultes FW. *European Non-Marine Molluscs, a Guide for Species Identification.* Goettingen, Germany: Planet Poster Editions, 2012.

Wheeler Q. *Species, Science and Society: The Role of Systematic Biology*. London: Routledge, 2023.